Metrology of Reflector Antennas: A Historical Review

Jacob W. M. Baars

Max-Planck-Institut für Radioastronomie
53121 Bonn, Germany
Priv. Prümer Wall 8
53359 Rheinbach, Germany
Tel: +49-2226-5905
E-mail: jaap@jacobbaars.de
Dedicated to the memory of Albert Greve,
metrologist extraordinaire

Abstract

The emergence of radio astronomy, space research, and satellite communication after World War II created great activity in the design and construction of reflector antennas of increasing size and precision, compared to the small radar antennas of the war period. With few exceptions, the reflectors consisted of a set of panels, typically a few square meters in size, that were supported on a backup structure. To be an effective reflector, the shape needs to obey the prescribed contour with a precision of about one-twentieth of the shortest operational wavelength. This was achieved with the aid of a continuously improving array of metrology methods, from the original geodetic theodolite-tape to current laser-trackers, digital photogrammetry, and radio holography. We review the historical development by summarizing the different methods and illustrating their applications with examples, mainly from the field of radio astronomy. It is here where the largest and most precise reflectors have been installed, and metrology has been pushed to a level where a reflector of 100 m diameter can be realized with a surface error of about 250 µm, and a 12 m diameter submillimeter telescope with an error of about 10 µm. The reference list is not exhaustive: it covers major papers of a general nature and detailed descriptions of the examples presented in the text. Table 1 provides a list of the acronyms used in the paper.

1. Introduction

When Grote Reber [1] designed his 10 m diameter parabolic reflector in 1936, his plan was to observe the sky at the highest possible frequency. He believed that the radiation from the region around the center of the Galaxy, discovered in 1932 by Karl-Guthe Jansky [2], would be of thermal origin, and hence would increase in intensity with increasing frequency. He thus started his observations at 10 cm wavelength, the shortest wavelength
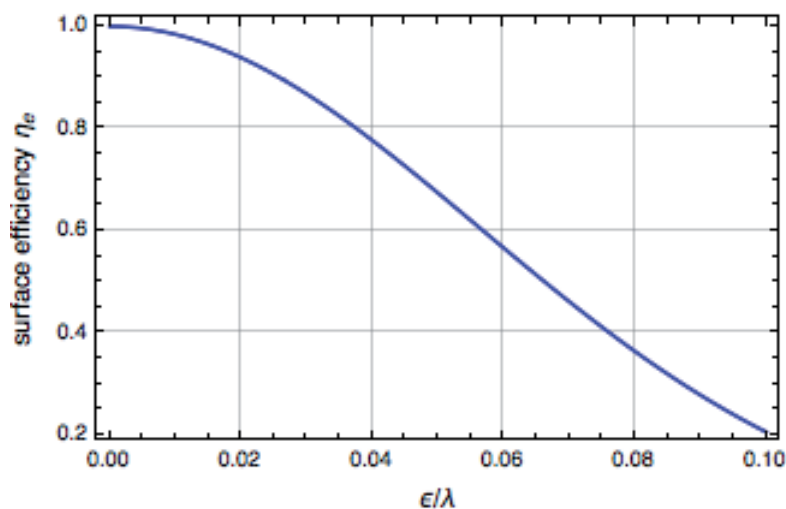

Figure 1. The "Ruze" curve shows the "surface scattering efficiency," η_S, as a function of the surface rms error, ε, normalized to the wavelength, λ.

where electronic components were available at the time. How precisely should his reflector have represented a paraboloid? He applied the criterion due to Rayleigh and used in optics that the maximum deviation of the mirror should be less than one-quarter of a wavelength (positive or negative, thus half a wavelength peak-to-valley). If we assume these errors to be randomly distributed with a Gaussian distribution, the rms error would have to be less than about one-tenth of the wavelength. In 1952, John Ruze [3] published his "tolerance theory" of random errors in the reflector profile. We there found that an error of $\lambda/10$ rms leads to a loss of efficiency of 80%. Most users found this an unsatisfactory situation. A value of $\lambda/16$ is often considered the limit, where the efficiency is decreased to about one-half (Figure 1).

Eventually, Reber observed at about a 2 m wavelength, and his reflector could be considered perfect. However, if one wants to observe at the submillimeter wavelength of 0.35 mm, a surface rms error of $\lambda/16$ means a surface precision of 22 μm! This is close to the specification of 25 μm for the 12-m antennas of ALMA, the Atacama Large Millimeter Array in northern Chile [4]. To achieve such performance not only requires fabrication capabilities of high quality, but also measuring methods to demonstrate both the manufacturing precision and the setting of the reflector panels to the required precision on the telescope's structure. This involves metrology methods and instruments with an accuracy of better than 10 μm "in the field."

Most large reflector antennas have a surface composed of a number of surface panels, placed in concentric rings of trapezoidal panels on a supporting backup structure (BUS) by means of adjustable screws that we shall call adjusters. The overall precision of the reflector surface is the superposition of the following components of errors:

i) The manufacturing precision of the individual panels, indicated by ε_p ;

ii) The gravitational deformation of the panels and the supporting backup structure, ε_b ;

iii) The deformations caused by temperature differences in the structure and by wind forces, ε_T ;

iv) The accuracy of the adjustment of the panels by the chosen method of surface metrology, ε_a

It is reasonable to consider these error contributions to be independent from each other. The overall root-mean-squared (rms) reflector error, ε_R , can then be written as

$$\varepsilon_R = \sqrt{\left(\varepsilon_p^2 + \varepsilon_b^2 + \varepsilon_T^2 + \varepsilon_a^2 \right)} . \qquad (1)$$

Considering that the desired overall surface error should be less than about five percent of the shortest wavelength,

and assigning equal contributions to the four aspects above, we see that the desired measuring and setting accuracy must be of the order of two to three percent of the shortest wavelength. For a 25 m telescope operating at 10 cm wavelength, the measuring accuracy should be about 2 mm. For a 12 m submillimeter telescope operating at 0.3 mm, we would need 6 μm measuring accuracy, i.e., a half-millionth of the reflector's diameter. This is a formidable requirement, in particular if it has to be fulfilled in the field. There are several routes along which the problem has been attacked, and the purpose of this paper is to present a historical review of the methods and instruments that have been developed and applied over the lifetime of radio astronomy, about 75 years. The presentation will be descriptive and illustrated by selected examples with references to the original papers. Estler et al. presented an exhaustive general review of large-scale metrology with 133 references, not limited to reflector antennas, in 2002 [5].

Apart from the measurement and setting of reflector surfaces, other aspects of the construction and operation of large and accurate – and hence short-wavelength – reflector antennas can be discussed under the general designation of metrology. An obvious example is the pointing and tracking precision under operational conditions. Temperature variations and wind influence cause deformations in the structure, which lead to pointing errors that cannot be sensed by the encoders. In order to correct for these in real time, one has to install a sensor system with accompanying algorithms that determines the structural deformation, and provides correcting data to the pointing control system. Such active systems are known as Flexible Body Compensation (FBC) [6]. They include the use of Finite Element Analysis (FEA) in correcting deformation due to gravity and measured temperature differences in the structure, along with sensors for directly measuring structural deformations that lead to pointing errors. These aspects warrant a separate paper.

2. Classical Reflector Metrology: From Theodolite to Laser Tracker

There are very few radio telescopes with a continuous reflector, fabricated in one piece. A major example was the NRAO 36-ft mm-telescope, machined in the mid-sixties in one piece on a large lathe to an accuracy of about 100 μm. That was a factor of two worse than specified. Moreover, after assembly on Kitt Peak, it soon became clear that there were serious thermal problems. However, readjusting the surface was impossible. Eventually, the reflector was replaced in 1983 by a traditional paneled reflector of 12 m diameter [7]. The usual way to form the reflector is to divide the surface into a number of concentric rings, and to place individual surface panels, typically of one to two square meters in size on a backup structure through adjusters. This assures the possibility of adjustment of the composite surface to a desired contour. The panels are fabricated to a certain specification and their accuracy is checked in the shop before delivery. Sometimes, the

Figure 2. The support frame with two panels of the Millimeter Radio Telescope's surface in coordinate measuring machines. The measurement accuracy was <5 μm, and the average panel surface error was 27 μm.

machine with which the panel surface has been shaped is also used to measure the resulting surface, which involves the danger of overlooking systematic errors in the fabrication process. Modern, large coordinate measuring machines (CMM) allow the measurement of panels of several square meters to an accuracy of a few micrometers. This can be done for the measurement of single panels, or during the assembly of a number of small tiles on an intermediate support subframe [8]. An example is shown in Figure 2, where two panels of the IRAM 30-m mm-radio-telescope (MRT) were measured and adjusted on a joint subframe in a large coordinate measuring machine in 1979 [9]. A similar layout was used on the Large Millimeter Telescope (LMT) in Mexico with subframes of about 10 m^2 , each carrying eight panels. There, the original setting was done on a coordinate measuring machine in the shop. A check and fine adjustment just before mounting on the telescope was performed with a laser tracker [10].

The reflector surface normally will thus consist of a large number of panels, each with its own small-scale manufacturing error and possibly intermediate-scale deformation due to gravity and temperature, placed through adjusters on the backup structure (BUS) with a certain adjustment error. The backup structure itself will deform under the influence of gravity, wind, and temperature, leading to relatively large-scale errors. A metrology system is needed to determine the correct setting of the adjusters.

Often, the actual adjuster setting also considers *a priori* knowledge about the intrinsic deformation of the panels – for instance, warp – by applying small offsets. In the following sections, we review the "geodetic" and "mechanical" methods that have been applied for the measurement of panel setting and reflector surface precision.

2.1 Classical Geodetic Methods: Measuring Distance and Angle

The classical method is to measure angle and distance to a point on the surface from a point on the reflector axis, often the vertex, with theodolite and measuring tape. The tape is either laid along the surface or stretched between two points. In the latter case, a correction for the sag of the tape must be made. The angle measurement is sensitive to variations in the refraction along the path, which can be significant on large reflectors. Greve performed the original setting of the Effelsberg 100-m telescope with this method, and achieved an uncertainty of < 1 mm in the final calculated rms surface error [11]. Using the same method, he set the original surface of the 30-m millimeter telescope on Pico Veleta to 150 μm [12]. These are among the best-ever values reached with this method, and they involved very careful and cautious measuring and attention to outside influences, such as temperature and humidity. The tape measurement can be avoided by measuring two angles from positions on the axis a known distance apart (Figure 3). This introduces twice the refraction variations in the sight line, while the error in tape measurement translates only for a small part into a vertical setting error for reasonably flat reflectors. This measurement will thus be slightly less accurate. An advantage is that it can more readily be used on a reflector pointing outside the zenith. This scheme was applied in 1966 with an alignment telescope positioned along the reflector axis and a set of pentaprisms stacked along this axis and pointing at the concentric rings of targets on a 30 m communication ground station, and achieved a precision of 0.5 mm [13]. At the Parkes radio telescope in Australia, a rapid and automatic method was developed whereby targets reflected in a mirror set at known angles were photographed. Measurements could be made at the operating elevation angle with the goal of removing structural deformations due to gravity, wind and temperature variations. The achieved accuracy was about 1 mm rms [14],
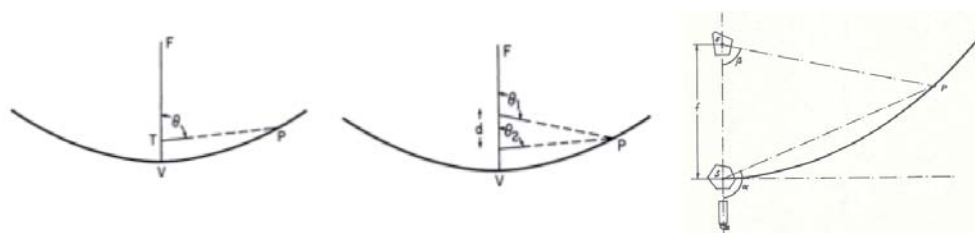

Figure 3. The "classical" methods with theodolite (θ) and tape (TP) (left); "two-angle" with known d (center); using two pentaprisms (right).
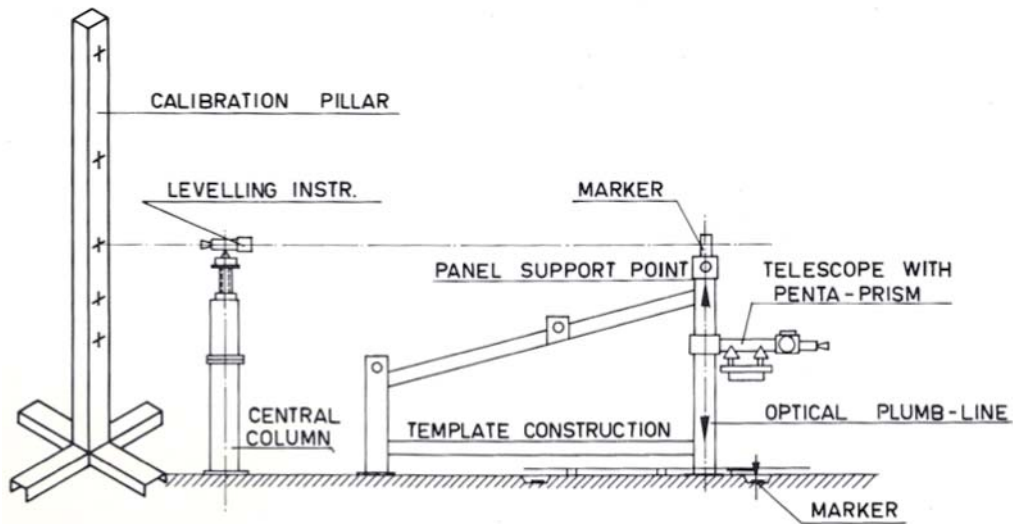
Figure 4. The measuring system used during assembly of the Westerbork Synthesis Radio Telescope dishes. The setting of the template points for the support of the reflector surface panels was done with respect to the calibration pillar and markers on the floor.

An alternative geodetic method applies an automatic level instrument, as, for instance, in the assembly of the reflectors of the Westerbork Synthesis Radio Telescope (WSRT) in the Netherlands. The surface panels and backup structure of the 14 dishes of this array were assembled in a template that was placed in a temperature-controlled assembly hall (Figure 4). The template provided support pins for the panels at precise height and radial coordinates. These were set radially by an optical plumb line, a telescope with attached pentaprism, to markers on the floor, and in height by an automatic level instrument in comparison to a calibration pillar with markers. After the panels were connected to form the reflector surface, but before they were attached to the backup support structure, the surface was measured with the level at several hundreds of points, and adjustments were made by shimming where needed. The accuracy of the method was about 0.1 mm: the reflectors showed a final rms of 1.5 mm, a factor of three better than the original specification [15]. Radiometric measurements at several wavelengths confirmed the overall reflector precision.

2.2 Advanced Geodetic Instrumentation

In the nineteen seventies, new distance and angle measurement instruments were developed that were based on lasers. Early versions of an instrument based on the principle of "laser-ranging" were presented by Payne [16] at NRAO in 1973, and by Greve and Harth [17] at the Max-Planck-Institut für Radioastronomie (MPIfR) in 1984. The MPIfR instrument was developed for the adjustment of the 30-m Millimeter Radio Telescope (MRT). The principle is shown in Figure 5. To avoid atmospheric fluctuations, the light was sent through a closed duct that could be moved over the surface. At the end the target, a retro-reflector returned the light to the theodolite for the measurement of the distance, r, while a diode array measured the variation in height of the surface, Δh, with respect to the theoretical value set by the angle θ. It showed a measuring accuracy of about 50 μm rms, and was used during the initial setting of the surface of the Millimeter Radio Telescope in 1982. The instrument did not come into routine use because of problems with the laser attachment to the theodolite, which would have required significant changes to the layout. Hewlett Packard introduced the laser-interferometer, which enabled the measurement of changes in the distance to a target at distances of the order of ten meters with an accuracy of one in a million. This instrument was used in the metrology
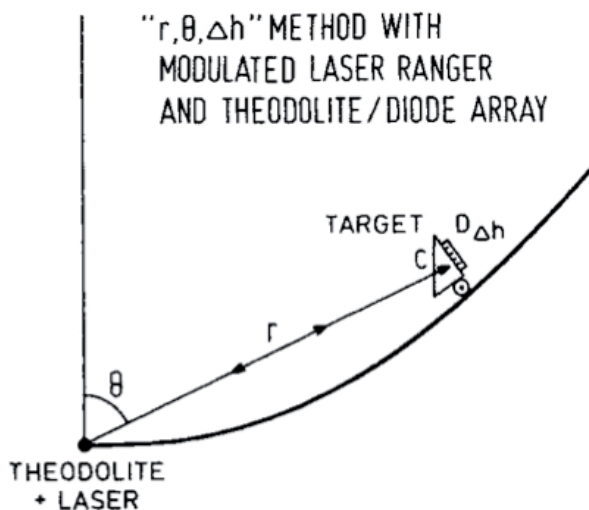

Figure 5. The principle of the laser ranging and height measurement of the reflector of the MPIfR/ IRAM 30-m millimeter telescope.
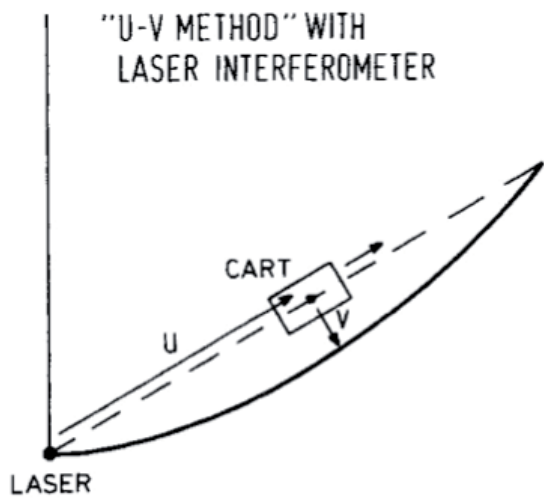
Figure 6. The principle of the laser-interferometer measurement of the UK/NL James Clerk Maxwell Telescope's 15-m submillimeter-telescope.

system proposal for the James Clerk Maxwell Telescope, a 15-m submillimeter telescope on Hawaii (Figure 6). A cart with a retro-reflector was pulled along a beam from center to reflector edge, and continuously measured the changes in the coordinates, u (radius), and v (depth), from which the coordinates of the surface can be derived [18]. Tests in the laboratory indicated a measuring accuracy of ~20 μm rms over ~10 m distance. Deployment on the telescope showed some weakness in the mechanical system and an unexpected sensitivity to vibrations. Routine use was also not realized. It seems fair to note that the principles and experimental realizations of both these instruments were original, and showed the feasibility to achieve the stated use. However, the instruments were obviously not engineered and fabricated to the level where field operation could

be assured. Originating in physics/electronics research laboratories, they lacked the detailed engineering that industrial engineers could have provided. Both groups decided to abandon their methods and switch to applications of radio holography, to be described below, which by the early 1980s had caught the interest of radio astronomers.

Leica and Automated Precision Inc, (API) introduced the commercial laser-ranger integrated in a theodolite for a simultaneous measurement of both angle and distance to a target. Such an instrument is also called a *total station* or a *laser tracker*. The target contains a retro-reflector for the range measurement that is based on a phase measurement of a modulated laser beam. Current commercial laser trackers are routinely used for the measurement and setting of reflectors. The typical accuracy is 1 arcsecond in angle and $(10 + 5/m)$ μm in distance. The measurement is analyzed in real time, and allows the immediate adjustment of panel position. A great advantage of the laser tracker is that it will automatically follow (track) the target while it is moved over the reflector's surface, and data can be obtained at any position. Figure 7 shows the layout of the Leica Laser Tracker, and a picture of the instrument. A similar instrument, manufactured by Faro, was applied for the initial setting of the "European" AEM antennas of ALMA, whereby a surface accuracy of 35 μm rms was achieved on the reflectors of 12 m diameter. The measuring accuracy was estimated to be ~25 μm.

A further development was the Laser Scanner, also called Laser Radar, that operates without the need of targets. This enables the scanning of the reflector at varying elevation angles even during operation of the telescope. A Leica terrestrial Laser Scanner was used for a deformation study of the Effelsberg 100-m telescope in 2013. The elevation-dependent focal length could be
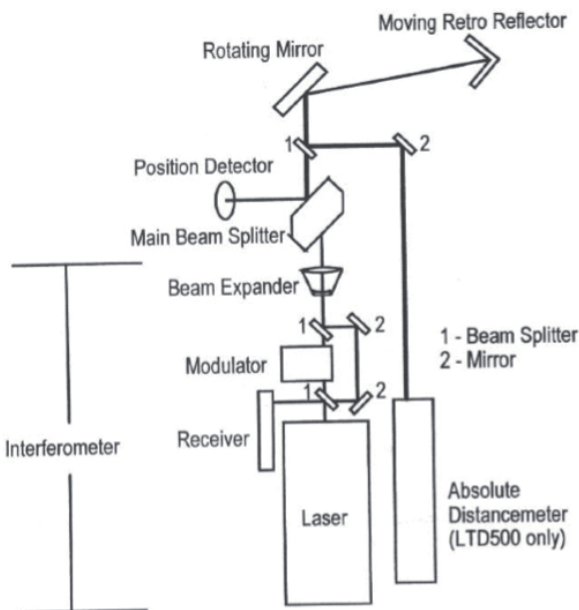

Figure 7a. The functional layout of the Leica Laser Tracker.
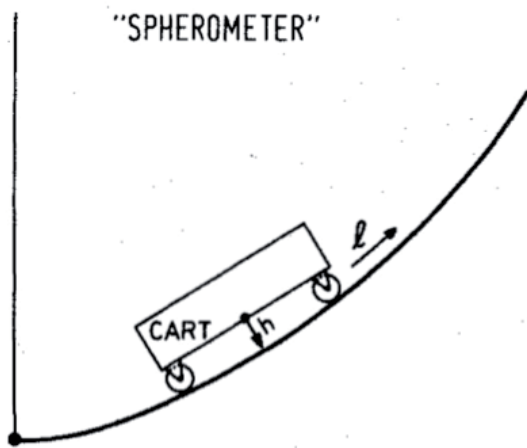

Figure 7b. A photo of the Leica Model 403 Laser Tracker.

Figure 8. The "spherometer" cart developed for the NRAO 36 ft millimeter telescope.

Figure 9. The "stepping bar" method applied at the NRAO 140 ft radio telescope.

monitored with an accuracy of better than 0.1 mm, while the standard deviation of the distance measurement over 50 m was about 1.3 mm [19]. The Laser Scanner/Radar appears particularly suited for large telescopes with remotely controlled adjusters of the surface panels. When sufficiently accurate scans of the surface can be obtained in quasi-real-time, the online correction of time-variable deformation, due to wind or temperature variations, becomes feasible. This is being planned for both the 64-m diameter Sardinia Radio Telescope (SRT) and the 100-m Green Bank Telescope (GBT). First tests on the Green Bank Telescope with LASSI (Laser Antenna Surface Scanning Instrument) based on the Leica ScanStation P40 led to a full design effort starting in 2020 [20]. First tests showed that deformations of about 55 µm can be determined in about five minutes if the wind speed is less than 4 m/s. The goal is to operate the system during daytime when the thermally induced deformations are most critical. A system for real-time surface correction, using six Digital Photogrammetric Units and three long-range Laser Trackers, is under development by Automated Precision Inc. for the 500-m Arecibo-type fixed reflector FAST (Five-hundred-meter Aperture Spherical Telescope) in China. The goal is to measure the absolute position of 1000 reflector panels to an accuracy of 2 mm within one minute of time [21].

2.3 Alternative "Mechanical" Methods

In the context of this historical review, we briefly mention a few original methods of surface metrology that were developed for a particular telescope or application. They have not penetrated into the arsenal of ubiquitous use.

2.3.1 The Spherometer

A measurement of local curvature and distance can be made with a spherometer, typically consisting of a cart
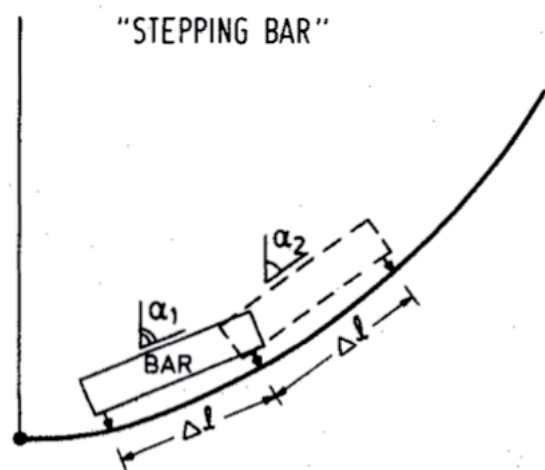
with an encoder on the wheels to measure the track, l, along radials on which a depth sensor measures the local depth, h (Figure 8). A twice-repeated integration delivers the profile of the reflector. Payne et al. [22] made experiments and demonstrated the feasibility of this method, achieving an rms accuracy of ~40 µm on the NRAO 36-ft mm-telescope.

2.3.2 The Stepping Bar

An alternative is the stepping bar of length Δl with an inclinometer, stepped along a radius and measuring distance and angle, α, step-by-step (Figure 9). Again, after integration of the data, the profile can be derived. Tests by Findlay and Ralston on the NRAO 140-ft telescope indicated that an accuracy of 40 µm could be reached on a proposed 25 millimeter telescope [23].

2.3.3 The Owens Valley Radio Observatory Method

A unique and sophisticated setup for measuring, accurately shaping, and fabricating highly accurate reflectors was developed by Robert Leighton at Caltech in the mid-seventies [24]. The goal was to develop an economical method to deliver a millimeter telescope for the Owens Valley Radio Observatory (OVRO) with a diameter of about 10 m, with good performance at 1 mm wavelength. The plan was to produce some four or five of these to establish a mm-wavelength array. Eventually, the fifth antenna, with a surface error of about 25 µm, was placed on Mauna Kea, Hawaii, as the Caltech Submillimeter Observatory (CSO). The method employs the geometric characteristic of a parabola and is shown in Figure 10. The ray of the HP laser-interferometer (LI) is deflected through 90° by the pentaprism, P, located on the slave cart, SC, that runs on the horizontal directrix template, T_D. It then hits mirror, M, on the cart, C, that moves along the parabolic template, T_C. The ray now travels to the focus, F, of the
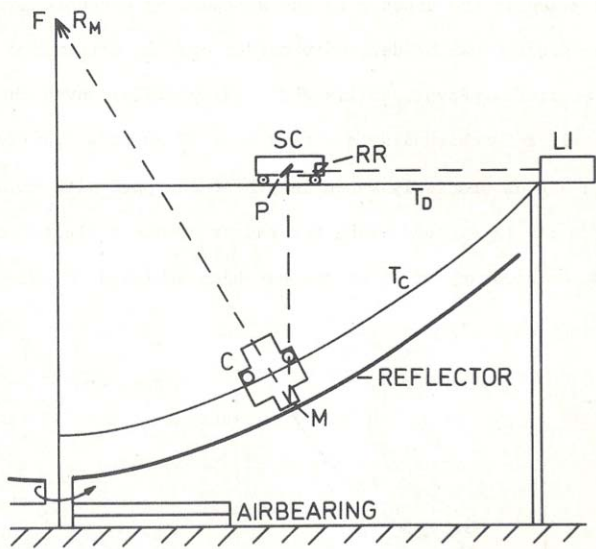
Figure 10. A sketch of the laser interferometer system devised by Leighton for the Caltech millimeter array.

parabola, where it is sent back on its path by the retro-reflector, R_M, via M to P on the slave cart. The path PMF must be constant for any position of M on a parabola. The returning ray is reflected to LI by the retro-reflector RR on SC. The template T_C is adjusted until the interferometer indicates a null: M hence lies on the parabola. With T_C accurately established, mirror M is replaced by a cutting head that brings the top layer of the aluminum honeycomb of the reflector into the parabolic shape. During the cutting, the entire reflector rotates about its axis, supported on an existing air bearing, used for the grinding of the Palomar 5 m optical mirror. After attaching the thin aluminum top sheet, the reflector is measured and small-scale fine cutting is applied to increase the precision. A detailed description was given by Woody et al. [25].

Most methods mentioned up to now require moving people and targets over the surface, and hence are essentially limited to measuring in the zenith position of the telescope. In operation, the antenna will occupy an intermediate elevation angle for most of the time, and it is highly preferable to set the surface to the best accuracy at such an elevation angle. We are thus interested in a non-contacting method to determine the reflector profile at an arbitrary elevation angle. We have mentioned above the Laser-Scanner that may enable correction for time-dependent structural deformation. We now direct our attention to an alternative method of quickly collecting sufficient data for the determination of the detailed shape of a reflector.

3. Photogrammetry

The three-dimensional shape of an object can be derived from the analysis of a number of photos taken by one or more cameras at a number of predefined positions. This process is called photogrammetry. In order to measure the detailed shape of the reflector, a sufficient number of targets are attached to the surface that are photographed under different angles by the camera(s). A small number of targets define the reference plane. From the photographic positions of the remaining targets, their three-dimensional position with respect to the reference plane can be derived. Comparing the data with the theoretical numbers for the perfect paraboloid delivers the "error distribution" of the actual reflector surface. In the case where the reflector is composed of individually adjustable panels, the measured deviations can be (partially) removed by adjusting the heights of the panels.

The first application of photogrammetry on a radio telescope occurred in late 1962, when John Findlay at NRAO in Green Bank arranged for the company D. Brown
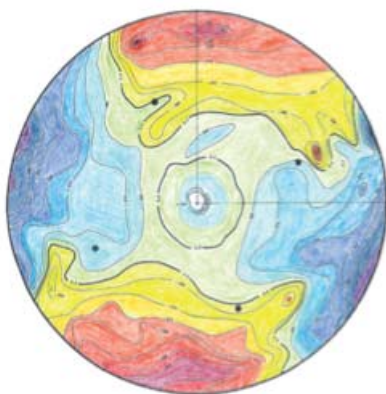

Figure 11a. A photogrammetric measurement of the 85-ft radio telescope at NRAO from a helicopter in 1962. This shows the map in the horizon-looking position: it shows a strong systematic astigmatic deformation. The contour interval is 1.5 mm; the rms deviations are about 3 (left) mm and 6 mm (right) (after Findlay [26]).
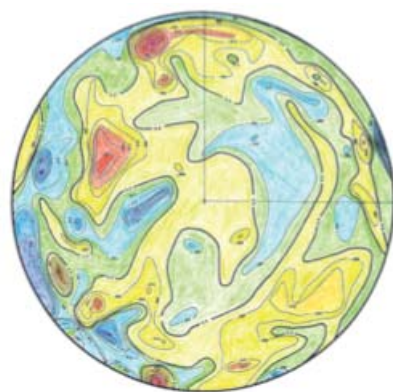

Figure 11b. This map in zenith position indicates a more random distribution of deviations. The contour interval is 1.5 mm; the rms deviations are about 3 (left) mm and 6 mm (right) (after Findlay [26]).

Figure 12a. Photogrammetry on an ALMA prototype antenna: a picture of the reflector with targets. The bright targets are calibration targets, while the lighter targets are the measurement grid.
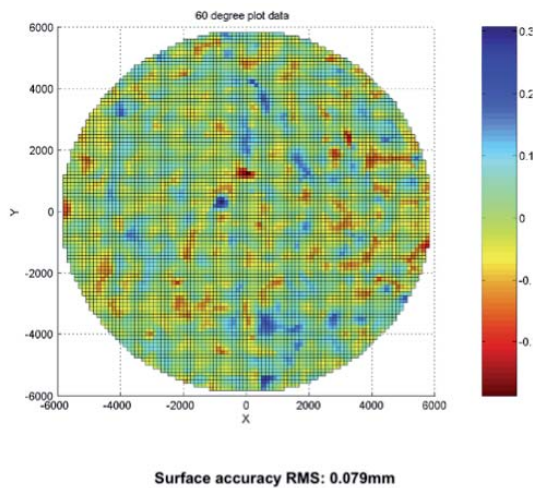

Surface accuracy RMS: 0.079mm

Figure 12b. Photogrammetry on an ALMA prototype antenna: a map of the surface deviations.

Associates of Florida to perform a photogrammetric survey of the 300-ft and 85-ft telescopes. About 300 targets were attached to the reflector surface of the 300-ft telescope. A special camera with an ultra-flat glass plate was mounted on a helicopter, and three photographs were taken at strategically chosen angles with respect to the reflector's axis at a distance of about 600 m. Data were obtained with the telescope pointed at 0°, 30°, and 51° zenith distance, respectively. Similar measurements were obtained of the 85-ft telescope in zenith and horizon positions. These results are shown in Figure 11. The rms measurement accuracy was estimated to be 4 mm on the 300-ft and 1.5 mm on the 85-ft telescope [26]. This was acceptable at the time, but clearly insufficient for the next generation of radio telescopes for short cm-wavelengths that require a surface precision of 1 mm or less.

In the two decades after the measurements of the NRAO telescopes, photogrammetry was barely used for the setting of radio telescopes reflectors, but the technology of the cameras and measurement machines along with software was steadily improved, notably by the Brown Company. By 1984, the company name had become Geodetic Services Inc. (GSI), and a new highly improved system, based on a microprocessor-controlled large film (23 cm × 23 cm) camera had been developed and marketed [27]. This system was used in 2000-2001 at the 300 m diameter spherical antenna of the Arecibo Observatory, after its second major upgrade, which was completed in 1997. Six cameras, mounted on the cable support towers of the antenna, were used to photograph the enormous area of the reflector. A total of 48 images were obtained to determine the positions of the 40,000 targets of 7 cm diameter that were attached to the surface. An rms value of 0.3 mm in each coordinate of the target was achieved, corresponding to an accuracy of 1 part in 1 million [28].

The emergence of digital cameras and advanced data-analysis methods has significantly widened the capabilities and areas of application of photogrammetry. Recently, there has been a growing use of the method for the measurement of large and highly accurate radio telescopes. The method is quick and relatively simple in its execution; it is non-contacting and hence applicable at varying antenna elevation angles. It thus is quite convenient in the early stages of antenna commissioning to remove the errors incurred in the initial setting of the surface panels. Being able to measure the reflector at several elevation angles provides data on the gravitational deflections in the structure, and enables a quantitative check on the quality of the structural finite-element model. For large telescopes, such as the Large Millimeter Telescope and the Green Bank Telescope, that rely on real-time adjustment of the reflector panels' positions to offset gravitational deflections, this is particularly advantageous.

In the early years of the twenty-first century, photogrammetry was used to characterize the two ALMA prototype 12-m antennas at the site of the VLA in New Mexico. Figure 12 shows one of the ALMA antennas with the calibration targets as bright spots and the measurement array of weaker dots. A result with an rms error of 79 μm is shown on the right side. The photographs were taken with a digital camera from a cherry picker that was moved through a number of positions at more than 5 m distance from the nearest edge of the reflector, to obtain between 100 and 150 images in a time of about 15 minutes. In the example here, the measured rms error of consecutive setting iterations converged from 400 to 70 micrometers in seven iterations. By making photos at several elevation angles between 5° and 90°, accurate data could be derived for the change in focal length and the stability of the focus with varying temperatures [29].

Table 1. Acronyms

AEM	Alcatel-European Industrial Engineering-MT Mechatronics
ALMA	Atacama Large Millimeter Array (Chile)
API	Automated Precision Inc.
BUS	BackUp Structure
CMM	Coordinate Measuring Machine
COMSAT	Communications Satellite Corporation
CSO	Caltech Submillimeter Observatory
CSIRO	Commonwealth Scientific and Industrial Research Organisation (Australia)
ESA	European Space Agency
ESO	European Southern Observatory
FAST	Five-hundred-meter Aperture Spherical Telescope (China)
FBC	Flexible Body Compensation/Control
FCRAO	Five College Radio Astronomy Observatory
FEA	Finite-Element Analysis
FEM	Finite-Element Model
FT	Fourier transformation
GBT	Green Bank Telescope
HHT	Heinrich Hertz Telescope
HPBW	Half-power beamwidth
INAOE	Instituto Nacional de Astrofísica Óptica y Electrónica (Mexico)
IRAM	Institute for Radio Astronomy at Millimeter-waves
ITALSAT	Italian (Ka-Band) Satellite
JCMT	James Clerk Maxwell Telescope
JPL	Jet Propulsion Laboratory
LES	Lincoln-laboratory Experimental Satellite
LMT	Large Millimeter Telescope (Mexico)
MIT	Massachusetts Institute of Technology
MPIfR	Max-Planck-Institut für Radioastronomie
NAIC	National Astronomy and Ionosphere Center
NASA	National Aeronautics and Space Administration
NRAO	National Radio Astronomy Observatory
OOF	Out-Of-Focus
OVRO	Owens Valley Radio Observatory
SKA	Square Kilometre Array
VLA	Very Large Array
WSRT	Westerbork Synthesis Radio Telescope

Later photogrammetry measurements by Hills and Schwab [30] indicated from repeated measurements an rms error of a measurement of the reflector of between 20 μm and 30 μm. This was about equal to the surface specification (25 μm, goal 20 μm). At this requirement level, photogrammetry is thus not yet a viable method for final panel adjustment. However, it offers a relatively easy and fast solution for initial measurement and setting. Interestingly, the accuracy was sufficient to show a systematic spherical aberration in the surface of both the "European" and "American" prototype antennas. Coincident with this finding, an error in the holography software was identified by Robert Lucas that causes such an aberration (see below). Indeed, the antennas had previously been set with the erroneous holography package, thereby introducing the systematic error.
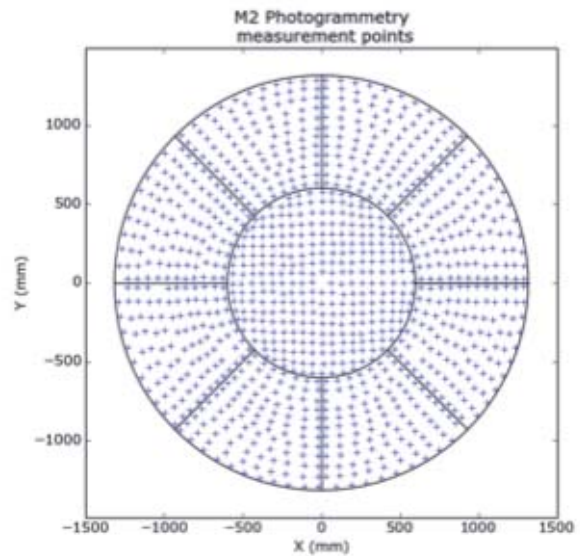

Figure 13a. Potogrammetry on the Large Millimeter Telescope subreflector, showing the sampling grid.

Figure 13b. The measurement setup for potogrammetry on the Large Millimeter Telescope subreflector. The camera (upper left) was moved to measure several hundred positions in three dimensions. Calibration bars are visible in the lower-left corner.

The Large Millimeter Telescope subreflector (diameter 2.5 m) was measured in the shop with both a laser tracker and photogrammetry [31]. The measured rms deviation of the hyperbolic surface was about 27 μm with the laser tracker and 24 μm with photogrammetry. Difference surface maps indicated a residual measurement rms error of 15 μm - 20 μm for the laser tracker and 10 μm - 12 μm for photogrammetry at these short distances in a laboratory environment. While this was a very good result, the stable laboratory environment in which the measurements were taken undoubtedly helped it. A measurement of an exposed telescope will suffer from environmental effects, such as wind, temperature, and humidity.

Photogrammetry has recently returned on the scene for the measurement of large telescopes, notably the 50-m
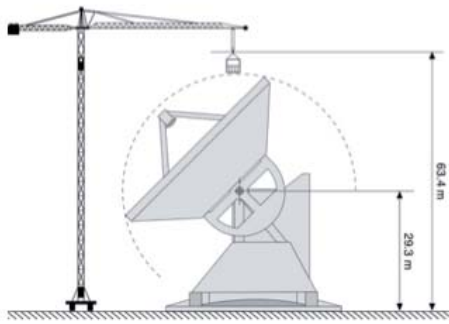
Figure 14a. The setup for photogrammetry of the Large Millimeter Telescope reflector. The crane carries the camera (upper left).
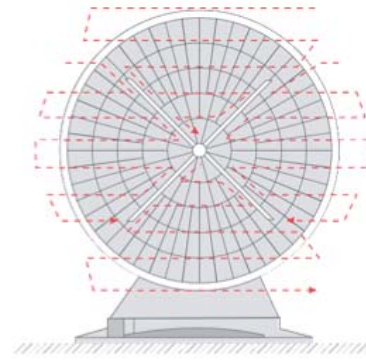

Figure 14b. The measurement pattern for photogrammetry of the Large Millimeter Telescope reflector.
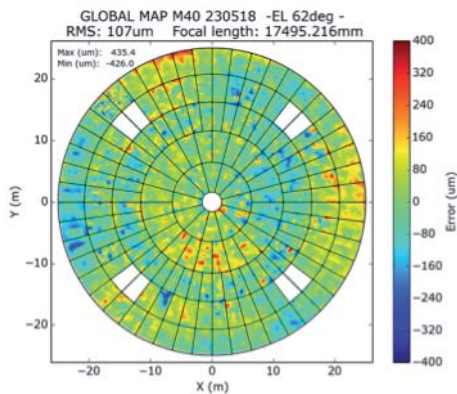

Figure 14c. The map of surface deviations indicates an overall rms of 107 μm for the Large Millimeter Telescope.

Figure 14d. A photo of the Large Millimeter Telescope.

Large Millimeter Telescope (LMT) in Mexico and the 64-m Sardinia Radio Telescope (SRT). Both telescopes employ a paneled surface supported on remotely controlled adjusters. A first use of these is the correction of elevation-dependent gravitational deformations on the basis of Finite-Element Model (FEM) predictions. Eventually, real-time thermal- and wind-induced deformations might be corrected with the adjusters. Next to the Large Millimeter Telescope on its 4600 m high site is a 60 m tall tower crane that enables the relatively easy execution of photogrammetric reflector surface measurements (Figure 14). From repeated measurements under stable weather conditions, an rms measurement error of about 70 μm has been derived [32]. After applying the surface corrections with the remotely controlled adjusters, the overall reflector showed an rms error of about 100 μm. There appears to be room for improvement, in particular with a more accurate radio-holography surface measurement, to be discussed below.

The capability of photogrammetry to measure and monitor structural deformation in a telescope is well illustrated in the study by Subrahmanyan of the 22-m diameter Cassegrain antenna of the Australia Telescope Compact Array [33]. Not only the large-scale deformation of the main reflector surface but also displacements of the subreflector and its quadripod support structure were measured at a number of antenna elevation angles. The relative positions of the targets on the structure could be measured with an accuracy of about 1:500,000, while the absolute position was determined to 1:60,000. Displacements of the subreflector of about 0.1 mm could be reliably determined. At the SRT on Sardinia, Italy, photogrammetry has been extensively used during on-site construction, erection, and alignment. A detailed comparison was made between Finite-Element Models and photogrammetric results [34]. Photogrammetry of the reflector suggested measuring errors ranging between 30 μm and 90 μm rms. This probably reflects the time-varying atmospheric situation between measurements. There are plans to use real-time photogrammetry for on-line deformation correction through the panel adjusters. The contractor, COMSAT, used photogrammetry for the demonstration of the surface specification during the delivery procedures of the Green Bank Telescope (GBT) in June 2000.

Table 2 contains both the measurement accuracy and the actual reflector accuracy (rms). The *measurement accuracy* is often estimated by taking the difference of two or more consecutive measurements. In other words, it

Table 2. Photogrammetry of Radio Telescopes

Institute	Location	Telescope	Diam. (m)	Accuracy (µm) Measurement	Accuracy (µm) Surface	Data	Year	Ref.
NRAO	Green Bank	85-ft	26	1500	3000	Plate	1962	26
NAIC	Arecibo	Sphere	300	500	5000	Film	2001	28
ALMA	New Mexico	Vertex	12	20	30	Digital	2005	30
CSIRO	Australia	ATCA	22	50	200	Digital	2004	33
INAF	Sardinia	SRT	64	–	<300	Digital	2015	34
INAOE	Mexico	LMT	50	50	150	Digital	2018	32

shows the *repeatability* of the measurement setup. Clearly, for a reliable determination of the reflector accuracy, the measurement accuracy must be significantly smaller than the actual reflector deviations. From the literature, it is not always clear whether the quoted accuracy is the repeatability or the overall reflector error. In any case, it is preferable to perform an independent check on the significance of the result. A convenient way is the measurement of the aperture efficiency at a few high frequencies to derive the reflector rms error [3].

Clearly, the capabilities of photogrammetry have increased enormously since 1980. The technique can now usefully be applied to radio telescopes of the highest precision. These very accurate telescopes, operating at millimeter wavelengths, were designed and built since the early seventies. Part of the design challenge was the development of methods and equipment for the final measurement and adjustment of the reflector surface with an accuracy well below 100 µm. As we have seen, the "classical" methods were not capable of achieving this, and photogrammetry is not yet competitive in view of the requirements. A natural approach was to search for a measuring method that is close to the "normal" use of the telescope, e.g., using cosmic radio sources and radio-astronomy equipment (receivers). Such a solution was eventually found. It goes by the name of "radio holography." It is currently the most accurate and widely used technique for the measurement of radio-telescope reflectors. We summarize the development of radio holography in the next section.

4. Radio Holography

In the classic text, *Microwave Antenna Theory and Design*, published in 1949 in the MIT Radiation Lab Series, the author, S. Silver, discusses the Fourier transform (FT) relationship between the field distribution in amplitude and phase over the aperture of the antenna and the far-field radiation pattern, also in amplitude and phase. The relation is reversible, and hence the aperture-field distribution can be recovered if one has a complete knowledge of the radiation field, both in amplitude and phase. Silver then notes: *"in practice, the radiation pattern is only known in power and the aperture distribution cannot be determined uniquely."* In 1966, Roger Jennison wrote a pocket book, *An Introduction to Radio Astronomy* [35]. In an appendix, he pointed to the same Fourier transform relationship and mentioned: *"this relation may be reversed to give the field in the aperture plane in terms of the directivity pattern (in amplitude and phase)."* Remarkably, although interferometry was extensively discussed in his book, he did not mention the use of an interferometer to record both the amplitude and phase of the radiation pattern.

The January 1966 issue of the *IEEE Transactions on Antennas and Propagation* contains a paper entitled "Measurement of the Complete Far-Field Pattern of Large Antenna by Radio-Star Sources" by P. G. Smith of the Research Triangle Institute in Durham, NC, USA [36]. In this paper, the complete theory of using an interferometer – the additional antenna delivering the needed reference signal – for the measurement of the radiation pattern of an antenna is presented. This paper went unnoticed by the radio-astronomy community, although the present author referred to it in two papers, also in the *IEEE Transactions*, in 1972 and 1973. The 1972 paper [37] presented an interferometric measurement of the Dwingeloo Telescope antenna pattern at 21 cm wavelength. In a private comment on that paper, Barry Clark of NRAO, Socorro, suggested to the author to use the phase information from the pattern measurement to derive the shape of the reflector. Unfortunately, we had not recorded the absolute phase during those measurements, and we missed the chance to be the first to demonstrate the feasibility of *radio holography*. Around this time, Clark made the same suggestion to John Findlay, who was leading the design studies for a 65 m diameter Millimeter Telescope [38]. Two 1971 papers by Bates and Napier extensively treated the theory and experimental confirmation of the *holographic approach to radiation pattern measurements* [39, 40]. These appear to have escaped the attention of radio astronomers, probably because the aspects of measuring the reflector shape were not explicitly mentioned in this work. In the early seventies, Jack Welch, who was at the time working with S. Silver at Berkeley, mentioned the method to his PhD student Richard Hills, but it did not result in an experiment on the Hat Creek Interferometer. Upon his return to Cambridge, UK, in 1974, Hills suggested the method to Martin Ryle. Scott and Ryle used the 5-kilometer synthesis telescope in Cambridge, UK, to measure the pattern of
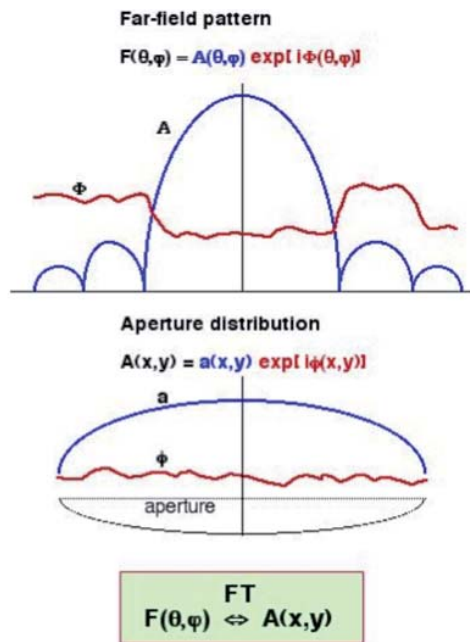
Figure 15a. The principle of deriving the aperture distribution through Fourier transformation of the far-field radiation pattern.

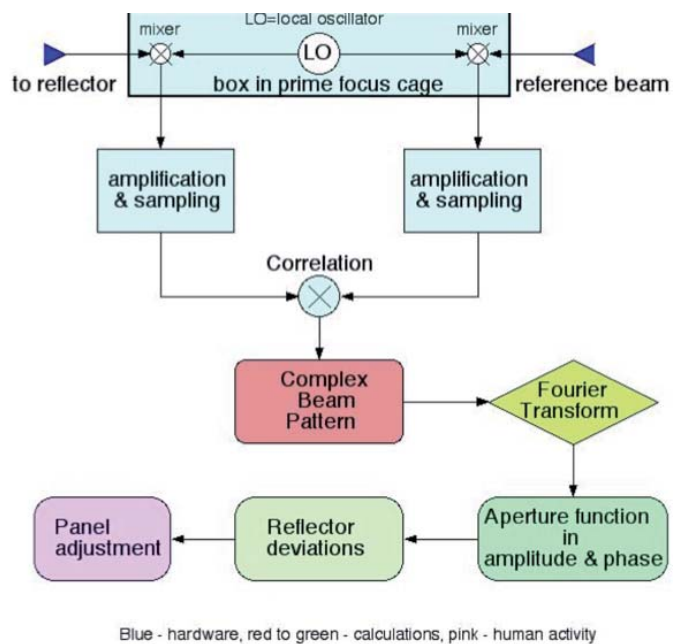Blue - hardware, red to green - calculations, pink - human activity

Figure 15b. A block diagram of the components of a holography system.

four of the eight antennas of the array, in both amplitude and phase, while using the other four array elements as reference sources. It demonstrated the practical feasibility of the method, and was published in 1977 [42]. Already in 1976, Bennett and colleagues at the University of Sheffield, UK, had published a ground-braking paper entitled "Microwave Holographic Metrology of Large Reflector Antennas" [41]. This paper did arouse the interest of radio astronomers, and builders of radio telescopes and ground stations for deep space and satellite communication. A few years later, the Sheffield group added to their theoretical work a measurement of the UK Chilbolton 25-m antenna using the beacon at about 11 GHz on the ESA "Orbiting Test Satellite" (OTS). Although the principle obviously occurred to others, it was the papers by Bennett et al. and Scott-Ryle that inspired a growing activity in the radio-telescope and space-exploration communities towards the application of radio holography for the measurement and setting of the reflectors.

The term r*adio holography* is generally used for any method to *measure the phase distribution of the reflector aperture field and to identify deviations from the expected function with local distortions from the prescribed profile shape of the reflector.* The information is obtained by Fourier transformation of the measured *radiation pattern both in amplitude and phase* by observing a radio source of high intensity at great distance. The method has been widely used to measure radio telescopes since the mid-1980s. Over the years, the method has been thoroughly analyzed and several variations have been introduced. In particular, the high requirement on surface precision of (sub)millimeter

telescopes has inspired detailed work in this field, especially in the control of systematic instrumental phase effects in practical situations where the signal source must be located at close range from the antenna under test. Measuring accuracies of better than 10 μm have been achieved for telescopes of 10 m - 30 m diameter.

The principle of holography is illustrated in Figure 15 on the left, and the basic block diagram is shown on the right. The antenna under test and a separate antenna that projects a steady reference beam receive radiation from a distant source. The test antenna is scanned in two coordinates over the source, and its output signal is correlated with the constant reference signal. The output of the correlator is the complex beam pattern of the test antenna with both amplitude and phase information over the angular region over which the pattern was sampled. Applying a Fourier transformation (FT) to this data delivers the distribution of the reflected field in the aperture of the antenna, both in amplitude and phase. For a point source in the far-field of the antenna and a perfectly parabolic reflector, the phase function of the aperture distribution will be a constant. Any deviation of the reflector from the ideal shape will project a phase change in the aperture field that we measure and identify with the reflector's imperfection. The spatial resolution of the aperture function is determined by the angular size of the measured beam pattern. Invoking the Nyquist criterion, a pattern measurement over an angle of n half-power beamwidths (HPBW) will yield a spatial resolution over the aperture of D/n, where D is the diameter of the antenna's aperture. There are a number of variations on this theme in the actual execution of a measurement.

4.1 Full-Phase Holography

The best method, which we call *full-phase holography*, is to use a separate antenna to provide the phase reference and to measure the pattern in full interferometric mode, i.e., in amplitude and phase. This is quite laborious, as one needs a phase-stable system with a separate antenna that must be sufficiently large to provide the needed signal-to-noise ratio. If one operates an interferometric array with a number of elements, life becomes quite easy, because all equipment, including the correlator and Fourier-transform software, is routinely available. Moreover the reference antenna is as big as the antenna under test and will deliver a very strong reference signal.

4.2 Near-Field Holography

If one is willing or forced to leave the far-field range offered by cosmic sources and satellite beacons, one can use an earthbound transmitter at a finite distance in the *near field* (Fresnel range) of the antenna. The straightforward Fourier transform cannot be applied before several corrections are made to the measured phase distribution to account for the geometrical effects of the finite distance to the source. These have, over time, been worked out. Currently, it is possible to make accurate surface maps with the aid of transmitters at only several hundreds of meters distance from antennas of 10 m - 20 m diameter at wavelengths of the order of one millimeter. In most cases, the full-phase mode is used, although in principle the phase-retrieval method is possible and has actually been applied.

4.3 Phase-Retrieval Holography

In this *phase-retrieval* method, introduced by Morris in 1985 [43], no reference signal is needed. The phase distribution over the aperture is estimated from the measurement of at least two power beam maps, obtained with different feed positions along the beam axis near the focus, through a laborious optimization algorithm. The method is often called *out-of-focus (OOF)* holography. In principle, this opens the way to use the available radio-astronomy receiver. However, the required SNR is an order of magnitude higher than in the full phase case. This will rarely be achievable with a cosmic source, but a strong satellite signal can offer the solution for which one often needs a special receiver because of the fixed frequencies of satellite beacons.

In the following sections, we review these alternative methods somewhat more closely and illustrate their characteristics with measurements on a number of radio telescopes.

4.4 Full-Phase Holography in the Far Field

Around 1980, the well-known water-vapor maser at 22 GHz in the Orion Nebula exhibited a giant outburst, with a flux density of about one million Jansky. For some time, the group at Max-Planck-Institut für Radioastronomie in Bonn, working on design and construction of the 30-m millimeter radio telescope (MRT), had been considering radio holography for the measurement and setting of the reflector surface panels. With the appearance of the Orion Maser it was determined that a sufficient signal-to-noise ratio would be available (assuming that the source would remain sufficiently strong over the time until the measurements would be done, a few years later), and a system for holography at 22 GHz was designed and built. It was decided to use full-phase holography. This implied that a reference antenna would need to be placed near or on the antenna under test. A very convenient arrangement is a receiver package with both receivers placed "back-to-back" behind the primary focus, with one feed in the focus illuminating the reflector, and the reference channel looking out to the source along the telescope's axis. The reference antenna is often just a broad-beam horn. Because of its wide antenna pattern, the signal remains almost constant despite the scanning of the antenna over the source during the measurement, and the small changes in its amplitude and phase can be accounted for in the data analysis. On the Millimeter Radio Telescope, a 2 m diameter reference reflector was mounted in the prime focus box, looking outward along the axis of the main reflector. This system achieved a measurement accuracy of about 35 μm in its first deployment, and the surface could be set to an overall precision of 85 μm in 1986 [44].

Still, very few cosmic radio sources are sufficiently strong to serve as useful signal sources for the requirements posed at short wavelengths. Extensive use has been made of the beacon signal of communication satellites, of which many transmit in the 11 GHz band. The signal of these is narrowband and strong, allowing a rather simple receiver system to be employed. The geostationary position of most satellites provides only one elevation angle for the measurement, its value being dependent on the latitude of the antenna. Several large antennas, both radio telescopes and communication ground stations, have been measured with a separate small reference antenna placed next to the test antenna. Some of the authors of the original paper [41] have offered a commercial service to measure large antennas. An example is the resetting of the surface of the 100-m diameter Effelsberg radio telescope in 1986 [45]. While the 22 GHz maser source in Orion significantly decreased in strength, the appearance in 1991 of the Italian ITALSAT satellite, with a beacon at 39 GHz at an elevation angle of 43°, was a godsend for the Millimeter Radio Telescope in Southern Spain. Over the next decade,
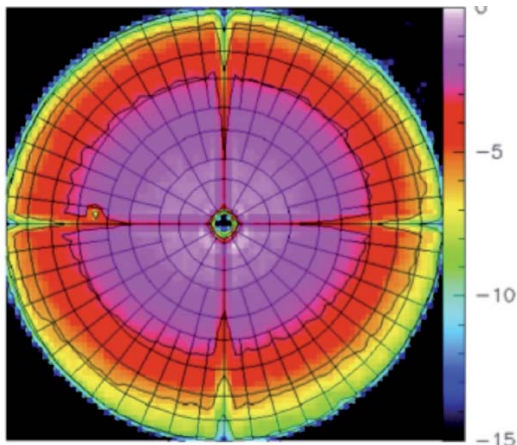
Figure 16a. An example of an ALMA antenna measured with "Astroholography" on Saturn at 84.2 GHz: the amplitude distribution.

Figure 16b. An example of an ALMA antenna measured with "Astroholography" on Saturn at 84.2 GHz: the phase map transferred to surface deviation, scale in μm. The resolved red patches of high deviation reflect problems with the adjusters, since corrected.

ITALSAT was used to improve the surface setting of the telescope [46]. A significant surface improvement after microwave holography of the Yebes 40-m telescope was reported in [47].

In some cases, several satellites at different azimuth angles have been used to obtain a surface map at a number of elevation angles. This is particularly interesting for the study of elevation-dependent gravitational deformations in the telescope's structure. The Green Bank Telescope was measured with the signals from three Intelsat transponders transmitting near 12 GHz. The 2200 surface-panel actuators were adjusted to yield an overall surface error of about 220 μm rms over the 100 m diameter reflector [48].

The Lincoln Experimental Satellites (LES 8 and LES 9), at a frequency of about 37 GHz, were used for the measurement of the 14-m FCRAO millimeter telescope in Massachusetts and the 12-m NRAO millimeter telescope on Kitt Peak in 1984. It was the sole source for the initial setting of the Heinrich Hertz (sub-millimeter) Telescope (HHT) on Mt. Graham, Arizona [49]. The geocentric orbit of these satellites, as seen from Earth, is an analemma (about the shape of the number 8), and covers a range in elevation angle from 30° to 65° at the telescope's location. Surface maps collected at these extreme angles thus provide information on the gravitational deformation of the reflector over this elevation range. Unfortunately, the LES satellites have ceased operation. However, there are several satellites with beacons in the 20 GHz - 50 GHz range that are suitable for the measurement of millimeter telescopes. For the measurement of submillimeter telescopes, operating at frequencies as high as 1 THz and requiring a surface accuracy of < 20 μm, satellite beacons are not readily available. Even the strongest celestial sources, the planets, do not always provide a sufficient signal-to-noise ratio for the relatively small antennas of 10 m - 20 m diameter.

As was pointed out before, the ideal signal source is a strong cosmic source of small angular extent (ideally,
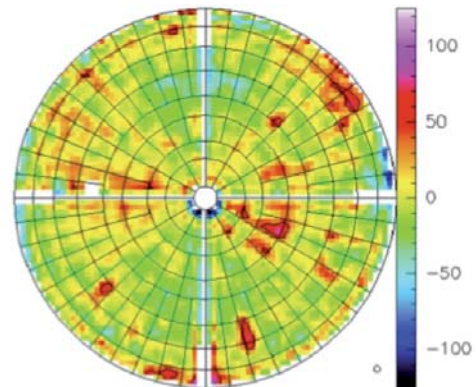
a "point source"), and for the antenna under test to be an element of an interferometric array of similar antennas. This was indeed the case with the first holography on a radio telescope by Scott and Ryle [42]. This situation also applies to the Atacama Large Millimeter Array (ALMA) in Northern Chile. ALMA consists of 50 highly accurate reflector antennas of 12 m diameter and a surface precision specification of 25 μm (goal 20 μm) rms [4]. The surface of each of the individual antennas has been measured and set with near-field holography at the Operations Support site at 3200 m altitude, to be described in the next section. Each completed antenna was transported along a road to the operations area at 5000 m altitude. There obviously is a need for checking the surface precision after transporting or storm situations and to monitor the surface quality over time. To this end full-phase holography, locally called *Astroholography*, is carried out with half of the antennas being simultaneously measured, while the other 25 deliver the reference signal. Planets radiate strongly at short mm-wavelengths, but their angular size is often too large for useful interferometry. If, in a fortuitous situation, a planet can be used, a highly accurate surface map with a high spatial resolution of the order of a few decimeters can be obtained. An example of such a measurement is shown in Figure 16, where an ALMA antenna was measured using Saturn as signal source at a frequency of 84.2 GHz (ALMA internal report). One can see strong deviations within a panel, which in this case were caused by problems with the panel position adjusters. If one uses point sources, such as quasars or masers, the lower source intensity limits the achievable spatial resolution to the order of one meter. This still gives a good impression of the overall stability of the reflector surface over time. Repeatability of a few micrometers has been obtained in this way.

The interest in the radio holography method has not been limited to radio astronomers. Space research organizations are dependent on powerful ground stations for control and data exchange with a growing arsenal of space probes and satellites at ever increasing distance. At
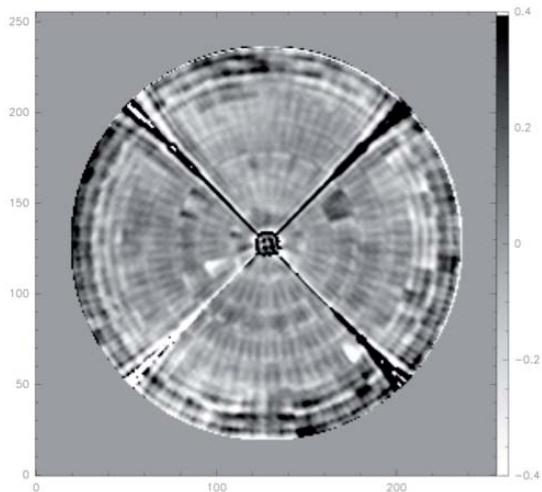
Figure 17a. Surface maps of the 30-m Millimeter Radio Telescope obtained from "full-phase" holography at 39 GHz: signal source in the far field, ITALSAT at 43° elevation angle.
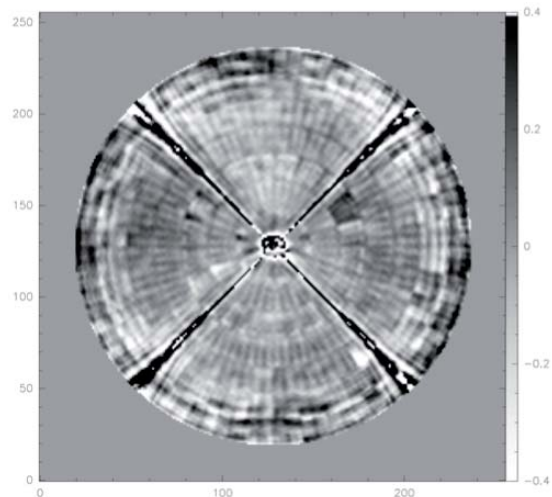

Figure 17b. Surface maps of the 30-m Millimeter Radio Telescope obtained from "full-phase" holography at 39 GHz: signal source in the near field, with the transmitter at 3 km distance and 11° elevation. The scales for Figures 17a and 17b are identical, the phase range is ±0.4 rad. The black panel at one-third out and 2 o'clock was offset by 1 mm for calibration purposes.

the Jet Propulsion laboratory (JPL), the operator of the network of NASA space research ground stations, the holography method was further developed with theoretical work by Rahmat-Samii [50] and development of a full-phase measurement system, capable of being ported between the antennas of the Deep Space Network. A description of the method, equipment and measurement results was presented by Rochblatt and Seidel [51]. Rochblatt summarized the extensive JPL activities in the JPL Descanso Book Series, Volume 10, Chapter 8 (downloadable from the JPL Web site) [52].

4.5 Full-Phase Holography in the Near Field

When neither a satellite beacon nor a cosmic source of sufficient intensity is available, it is necessary to take recourse to an Earth-bound transmitter. Among the first was a measurement of the Texas 4.9-m millimeter telescope on Mt. Locke at 2000 m altitude. There, a transmitter at 1700 m altitude and 12.9 km distance, close to the far-field distance of 13.8 km, provided the signal [53]. The frequency was 86 GHz and a measurement accuracy of 4 μm, based on repeated measurements, was reported. However, an Earthbound transmitter will, in most cases, be located in the Fresnel region *(near field)* of the antenna, which complicates the analysis of the measurements. Contrary to a source near infinity, such as a geostationary satellite (30000 km) or a cosmic source, the proximity of the source causes additional phase effects in the received wavefront that will have to be corrected in the data analysis. This requires knowledge of the distance to the source and the precise optical and mechanical geometry of the antenna. These disadvantages are offset by the strength of the transmitter signal and the simplicity of the receiver, being essentially monochromatic. Over time, the necessary corrections have been identified and worked into the analysis algorithms, and the method

can be used reliably for distances of only several hundreds of meters from an antenna of diameter of the order of 10 m, operating at short millimeter wavelengths. Morris presented an excellent review of the methods and results up to 1984 [54]. Figure 17, taken from a paper by Morris et al. [46], shows two surface maps of the Millimeter Radio Telescope, one taken with ITALSAT as the far-field source, the other with an Earthbound transmitter at the same frequency at only 3 km from the antenna. The two measurements were taken within a few days and show an excellent quantitative similarity, indicating the proper functioning of the near-field system. At that time, September 1998, the surface showed an rms error of 70 μm.

A full-phase system with a transmitter at about 800 m distance was used on the James Clerk Maxwell Telescope on Hawaii. This submillimeter telescope is placed in an astrodome with a thin Goretex membrane covering the opening, to reduce wind and temperature influences. Reflections on the membrane proved problematic, and led to a more elaborate system with two frequencies at 80 GHz and 160 GHz, each of which could be "chirped" to remove the spurious reflections. The final result is shown in Figure 18. In the phase map on the left, the surface panels were clearly resolved and some outliers were marked by the white or dark brown color. In the amplitude map, one can see illumination taper, weak diffraction rings from the edge of the subreflector, and the gaps between the panels [55].

In the case of the ALMA antennas, a measurement of the reflector with an accuracy of not worse than 10 μm is required. This was achieved with a full-phase near-field holography system. The transmitter, at a frequency of 100 GHz, was placed on a 50 m high tower at a distance
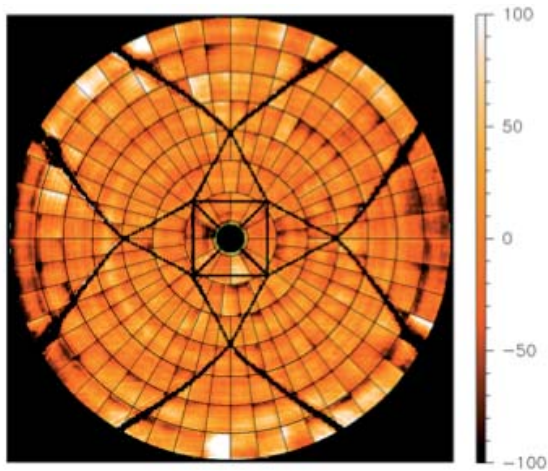
Figure 18a. A near-field full-phase measurement of the surface map of the James Clerk Maxwell Telescope in μm.
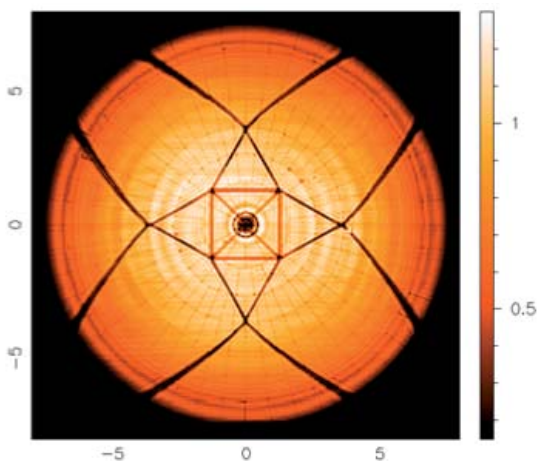

Figure 18b. The normalized amplitude of the aperture distribution corresponding to Figure 18a. The amplitude plot shows the outline of the panel gaps and the shadows of the intricate "octopod" subreflector support structure (R. Hills, personal communication).

Figure 19a. Near-field full-phase holographic maps of an ALMA antenna: the final surface map with an rms error of 11.9 μm.

Figure 19b. The difference between two consecutive measurements of the ALMA antenna with an rms error of 1.6 μm. Note the different intensity scales between Figures 19a and 19b, and also the blocked area (white) of the quadripod and subreflector, as well as two faulty panels that were removed from the data before analysis.

of about 300 m, providing an elevation angle of about 10°. As an example, Figure 19 (internal ALMA/ESO report) shows the surface map of one antenna together with the difference between two consecutive measurements, taken a few hours apart. The surface had an rms deviation from the perfect profile of 12 μm, while the difference map indicated a repeatability of better than 2 μm rms, and showed rather large-scale deviations. Small temperature effects or atmospheric fluctuations could cause these.

Similar measurements of the ALMA prototype antennas were presented by Baars et al. [56]. That paper included the detailed mathematics of the near-field method, and described the equipment, measuring routine, data analysis, and reflector-setting procedures. The pictures of Figure 20 show the experimental setup.
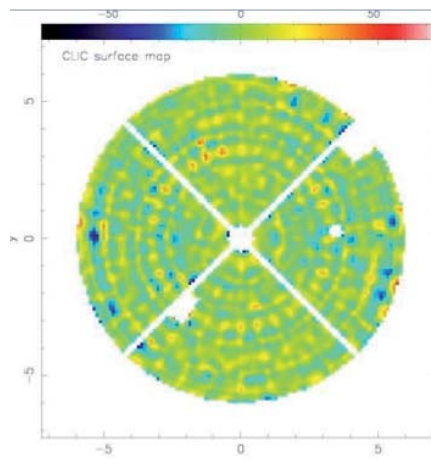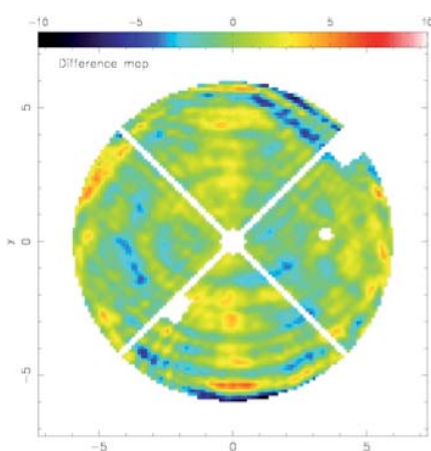
4.6 Phase Retrieval – "Out-of-Focus" (OOF) Holography

For those cases where the installation of a separate reference antenna is not possible or inconvenient, an alternative procedure, called phase-retrieval holography, was developed. Departing from an algorithm introduced in X-ray crystallography by Misell [57], in 1984 Morris [43] presented a method to retrieve the phase function from a pair of power beam maps taken by the antenna with the feed in two different axial locations. The method is also known as out-of-focus (OOF) holography. The required SNR is an order of magnitude higher than in the full phase case.

Figure 20a. A radio holography setup for the ALMA prototype antennas at the VLA site in New Mexico: the receiver feed in the prime focus box with the feed illuminating the reflector. Note the absorbent material around the feed to suppress multipath radiation.
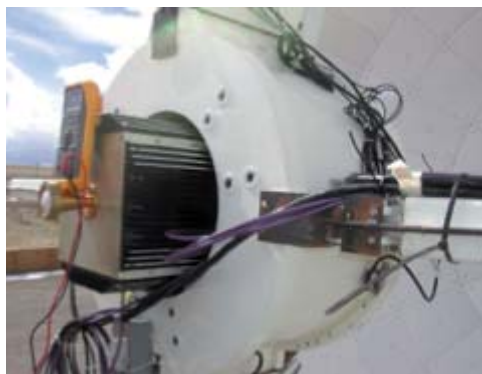

Figure 20b. A radio holography setup for the ALMA prototype antennas at the VLA site in New Mexico: the rear section of the receiver package with the reference horn on the left.

Figure 20c. A radio holography setup for the ALMA prototype antennas at the VLA site in New Mexico: the transmitter on a 50 m high tower pointed at the reflector. The VLA antennas are in the background.

In 1988 Morris et al. [58] successfully demonstrated the phase-retrieval method on the 30-m Millimeter Radio Telescope by measurements at 86 GHz with a signal source in the near field. Figure 21 shows a comparison between
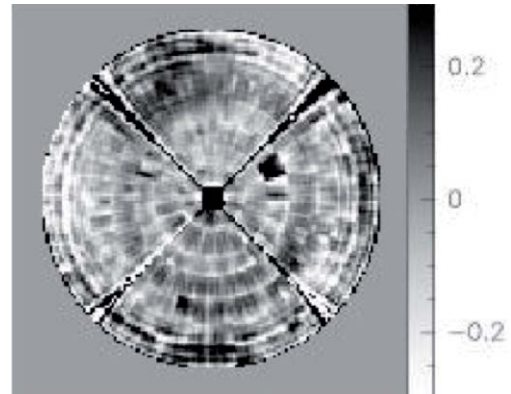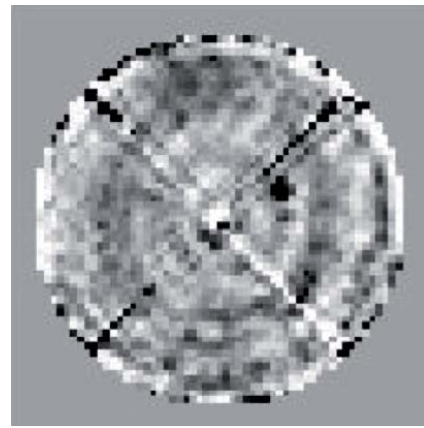

Figure 21. A comparison of phase retrieval (a) and full phase (b) measurement of the Millimeter Radio Telescope reflector. The dark panel under the upper-right quadripod shadow was purposefully offset by 1 mm. The map in (b) was measured at a higher spatial resolution, clearly visible in the plot.

surface maps obtained with phase-coherent and phase-retrieval measurements at 39 GHz from the ITALSAT satellite [46]. The similarity was quite good and numerically well within the estimated measurement accuracy.

The method was further developed by Nicolic and colleagues at Cambridge, UK [59]. By describing the surface errors as a linear combination of Zernike polynomials, the numerical inversion of the measured beam patterns led to the Zernike coefficients of the actual deformed surface. A measurement of the James Clerk Maxwell Telescope submillimeter telescope showed that large-scale surface errors could be reliably determined with a signal-to-noise ratio of 200, significantly smaller than required for the application of the Misell algorithm. The use of cosmic sources and standard astronomical receivers then became feasible, enabling the measurements of the surface shape at different elevation angles. This approach is restricted to relatively large-scale surface deviations, and will normally not be helpful for the setting of individual surface panels. The advantage to trace large-scale deformations in time by the operational astronomical system enables frequent correction of these errors, provided the surface panels are supported by remotely controllable adjusters. As mentioned
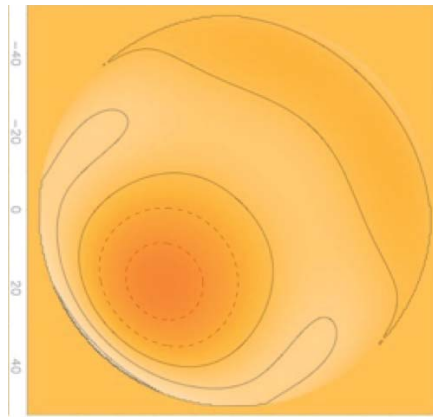
Figure 22a. A demonstration of the OOF method: the wavefront error resulting from a known deformation of the primary reflector. Contours are drawn at a surface interval of 275 μm. The scale is about ±1 mm.
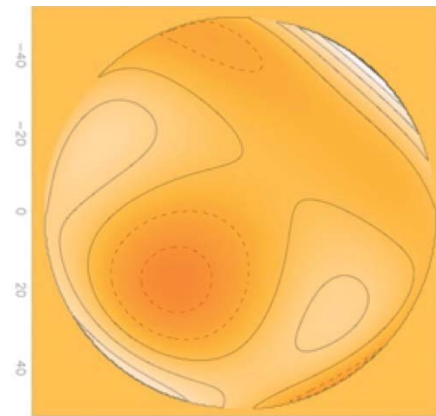

Figure 22b. A demonstration of the OOF method: the measured wavefront error using the OOF holography technique. Contours are drawn at a surface interval of 275 μm. The scale is about ±1 mm.

earlier, several recent large telescopes offer this possibility, and it was adopted for a fast measurement of the large-scale deformations of the 100 m diameter Green Bank Telescope (GBT) [60]. These deformations are caused by gravity, and change significantly with elevation angle. Temperature gradients in the structure also lead to deformations, and the relatively short time needed for a surface measurement (about 20 minutes) could enable "tracking" the slowly varying thermal effects in the structure.

A result of a measurement is shown in Figure 22. Here, a known deformation, shown on the right, was introduced into the surface, and the deformation map, derived from the OOF measurement, is shown on the left. The measurement was performed at 7 mm wavelength, taking about 30 minutes of time, and achieved an accuracy of about 70 μm rms [60]. It is a viable way to correct in quasi-real time large-scale surface deformations of large reflectors with remotely controlled motorized adjusters.

4.7 Shearing Interferometer

For the measurement of the Caltech Submillimeter Telescope, a method widely used in testing optical mirrors was adapted for millimeter wavelengths: the shearing interferometer, also known as the Twyman-Green interferometer. A functional drawing of the scheme is shown in Figure 23. For the description, we borrow from an earlier text by the author [63]. The paraboloid, P_1 re-images the primary reflector onto two flat mirrors, M_1 and M_2, via a beam splitter, BS. The beams reflected from M_1 and M_2 are recombined, and brought to the detector in the final focal plane via the off-axis paraboloid P_2. Mirror M_2 can be rotated about two axes perpendicular to the incoming wavefront. Because the primary reflector is imaged onto M_2, a rotation of M_1 is equivalent to a change in the pointing direction of the primary reflector. Seen from the detector in the focal point, the fixed mirror M_1 thus directs a beam towards the source, while the moving mirror M_2 scans a second beam to off-axis positions. The image mirrors M_1 and M_2 represent the elements of an interferometer as used in the holographic system described above. In this case, the focal plane field distribution is sampled off-axis by virtue of the moving mirror M_2. A Fourier transformation of the focal plane field distribution delivers the aperture field distribution. This measurement will thus provide the same information as the usual holographic interferometry. Because the relative phases of the two beams are present in the interferogram at the detector, only a single detector is needed, and even an incoherent detector such as a bolometer can be used. Because the primary reflector is imaged onto mirror M_2 and the wavefront from a point on the primary surface is sheared laterally by a rotation of M_2, the authors coined the name "shearing holography" for this measurement method. A full description of the method, along with experimental results, was presented by Serabyn et al. [64]. No wider use of this method has come to the attention of the author.
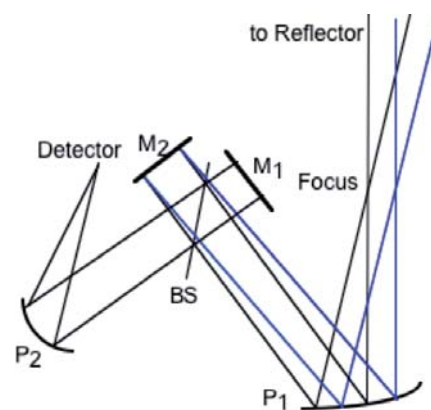

Figure 23. The layout of the shearing interferometer. P_1 and P_2 are off-axis paraboloids, BS is the beam splitter, and M_1 and M_2 are plane mirrors. M_2 can be rotated about two axes perpendicular to the incoming beam; the blue lines indicate an off-axis beam from M_2.

Table 3. Telescopes with reflectors measured by radio holography.

Telescope Location	Diam. (m)	Method	Source	Freq. (GHz)	Resolution (m)	Accuracy (µm) Measurement	Accuracy (µm) Surface	Ref.
Cambridge	18	FP-FF	CS-q	1.4	1.0	100	–	42
Texas mm	5	FP-FF	T	86	0.05	5	–	53
NRAO-AZ	12	FP-FF	S-LES	37	0.2	20	–	rep
NRAO-VLA	25	FP-FF	CS-q	5	1.4	300	–	rep
Onsala	20	PR-FF	CS-m	22	1.6	140	–	62
MPIfR-Effels.	100	FP-FF	S-OTS	11.5	0.5	50	500	45
IRAM-MRT	30	FP-FF	CS-m	22	0.7	25	75	44
IRAM-MRT	30	PR-NF	T	86	0.5	65	85	58
IRAM-MRT	30	FP-FF	S-Itals.	39	0.25	10	50	46
MPIfR-HHT	10	FP-FF	S-LES	37	0.1	<10	12	49
UK-JCMT	15	FP-NF	T	80/160	0.3	<10	25	55
ALMA-proto.	12	FP-NF	T	95		10	17	56
ALMA-Chile	12	FP-NF	T	95		<5	11	rep
Yebes-Spain	40	FP-FF	S	11.5	0.4	–	200	47
GBT - WVA	102	PR-FF	CS-q	43		70	–	59

Method: FP = full phase, PR = phase retrieval, FF = far field, NF = near field
Source: T =(local) transmitter, S = Satellite, CS = cosmic source, q = quasar, m = maser

4.8 Summary of Radio Holography

Radio holography has become the most widely used method for the characterization and optimization of paneled reflector antennas. The examples of the foregoing sections were meant to be indicative of the development and progress of the method. In the earlier days, the main purpose was the precise measurement and following adjustment of the panels of the reflector. This requires a rather high spatial resolution over the aperture, and hence a beam measurement over a substantial angle from the beam axis. For this the application of a full-phase system is advantageous. While a signal source in the far field of the antenna requires a minimum in corrective measures before the Fourier transformation to the aperture field, the complications of locating the source close to the antenna in the near field have been fully worked out and can routinely be applied to the data. A significant advantage of a near-field measurement is the shortness of the transmission path through the atmosphere and the resulting decrease in phase variations caused by atmospheric turbulence. More recently, large and highly precise radio telescopes, particularly those operating at (sub)millimeter wavelengths, include remotely controlled adjusters to align the surface panels to the desired surface. This offers the possibility of correcting known errors in real time, the obvious example being the counteraction of elevation-angle-dependent structural deformation due to gravity that can be calculated with the aid of a finite-element analysis of the structure. The major time variable deformation normally is caused by temperature gradients in the structure. The temperature field can be mapped by a set of strategically placed sensors in the structure. Introducing this in the finite-element model delivers the additional structural deformation that can be corrected by motorized adjusters [61]. Because the temperature field is predominantly large-scale, a surface map on this scale can be obtained by a relatively small holography beam map. For this procedure, a quick out-of-focus (OOF) beam map obtained on celestial signal sources has been shown to be feasible, as demonstrated on the Green Bank Telescope [60]. Depending on the temperature behavior over time, short OOF measurements could thus provide surface corrections in real time.

In Table 3, we summarize the major varieties of the holographic method, and list examples of telescopes at which they were applied together with the achieved accuracy and a reference, where available. Table 4 presents a timeline of the development and application of radio holography.

5. Conclusion

The holographic method has been the predominant means of measuring reflector antennas since the mid-eighties. Recent improvements in both digital photogrammetry and the application of flexible and accurate laser-scanners have become competitive alternatives, as illustrated in earlier sections. The choice of a particular method depends on the main purpose of the measurement activity. For instance, during assembly of the reflector, the placement of the panels can be monitored in real time by a laser tracker. We mentioned in Section 2.2 the plan to install a laser-scanner system on the Green Bank Telescope for continuous monitoring of wind and thermally induced deformations, and to make corrections to the panel positions in real time without the need to interrupt astronomical observations. In Section 3 we saw that photogrammetry

Table 4. Timeline of the Development of Radio Holography

1966:Smith – paper with full description of interferometric principle [36]

1971:Napier – Bates papers of holographic radiation pattern measurement with indications of application on reflector antennas [39, 40]

1973:Hartsuijker et al. – Complete antenna pattern of Dwingeloo telescope by interferometry; amplitude only, no surface map possible [37]

1976:Bennett et al. – basic full description of holographic method [41]

1977:Scott&Ryle – first use with cosmic source on Cambridge 1 mile array [42]

1983:Davis et al. – Texas mm telescope at 3.5 mm wavelength, 13 km range [52]

1985:Morris – theoretical paper on phase retrieval holography [43]

1985:Morris et al. – Millimeter Radio Telescope measurement with 22 GHz H2O maser cosmic source; full-phase with 2 m reference dish [44]

1985:Rahmat-Samii – simulation algorithms and application to JPL measurements [49]

1986:Godwin et al. – Effelsberg measurement with satellite source at 11 GHz [45]

1988:Morris et al. – comparison Millimeter Radio Telescope measurement with full phase and phase retrieval, includes the near field effects in phase retrieval [57]

1992:Rochblatt & Seidel – JPL system for NASA deep space network antennas [50, 51]

1994:Baars et al. – HHT submm telescope with LES satellite, accuracy <10 µm [48]

2001:Hills et al. - James Clerk Maxwell Telescope near field – full phase [55]

2002:Nikolic et al. – Out-Of-Focus (OOF) phase retrieval on submm James Clerk Maxwell Telescope [58]

2002:Morris et al. – review of several methods on Millimeter Radio Telescope over many years [46]

2005:Nicolic et al. – OOF holography OOF at 7 mm cosmic source on the Green Bank Telescope [59]

2004:Baars et al. – near field at 3 mm of ALMA prototype antennas [55]

2011:Hills et al. - ALMA, near field at 3 mm, production antennas, repeatability 2-3 µm

2011:Lucas et al. – ALMA "astro-holography" on celestial sources; in regular use.

is a versatile measuring method that enables quick results at different elevation angles to determine gravitational deformation. However, the obtainable accuracy is not (yet) sufficient for the most precise submillimeter telescopes. While further improvements in photogrammetry and laser-scanner technology will be achieved, it is likely that radio holography will remain the favorite method for radio astronomers. The similarity of the needed equipment with standard radio-astronomy receivers is advantageous, in particular when the antennas of multi-element arrays need to be measured, as for instance in the case of ALMA, the Square Kilometre Array (SKA), and the new generation Very Large Array (ngVLA).

6. Acknowledgement

7. References

1. G. Reber, "Cosmic Static," *Proc. IRE*, **28**, 1940, pp. 68-70.

2. K. G. Jansky, "Electrical disturbances apparently of extra-terrestrial origin," *Proc. IRE* **21**, 1933, pp. 1387-1398.

3. J. Ruze, "The effect of aperture errors on the antenna radiation pattern," *Suppl. al Nuovo Cimento*, **9**, 1952, pp. 364-380.

4a. A. Wootten and A. R. Thompson, "The Atacama Large Millimeter/Submillimeter Array (ALMA)," *Proc. IEEE*, **97**, 2009, pp. 1463-1471.

4b. J. G. Mangum, J. W. M. Baars, A. Greve, R. Lucas, R. C. Snel, P. Wallace, and M. Holdaway, "Evaluation of the ALMA Prototype Antennas," *Publ. Astron. Soc. Pacific*, **118**, 2006, pp. 1257-1301.

5. W. T. Estler, K. L. Edmundson, G. N. Peggs, D. H. Parker, "Large-Scale Metrology/An Update," *CIRP Annals*, **51**, 2002, pp. 587-609.

6. H. J. Kärcher, "Enhanced Pointing of Telescopes by Smart Structure Concepts Based on Modal Observers," *Proc. SPIE*, **3668**, 1999, pp. 998-1009.

7. M. A. Gordon, "*Recollections of Tucson Operations*," The mm-Wave Observatory of NRAO, Springer, Astrophysics and Space Science Library **323**, 2005.

8. H. Eschenauer, H. Gatzlaff, H. W. Kiedrowski, "Entwicklung und Optomierung hoghgenauer Paneeltragstrukturen," *Tech. Mitt. Krupp Forchungs Ber.*, **38**, 1980, pp. 43-57.

9. J. W. M. Baars, B. G. Hooghoudt, P. G. Mezger and M. J. de Jonge, "The IRAM 30-m millimeter radio telescope on Pico Veleta, Spain," *Astron. & Astrophys.*, **175**, 1987, pp. 319-326.

10. D. Gale, G. Hernández, A. Rincón, M. Sosa, A. León-Huerta, L. Cuevas, M. Álvarez, E. Sosa, D. Santos, C. Torres, E. Rios, "Delivery of 20-micron surface segments for the 50-meter LMT primary reflector," *Proc. SPIE Advances in Optical and Mechanical Technologies for Telescopes and Instrumentation III*, **10706**, 2018, p. 3810706.

11. A. Greve, "Metrology of the Effelsberg 100 Meter Radio Telescope," *Zeitschrift für Vermessungswesen*, **106**, 1981, pp. 308-315.

12. A. Greve, "Reflector surface measurement of the IRAM 30-m radio telescope," *Int. J. Infrared and Millimeter Waves*, **7**, 1986, pp. 121-135.

13. C. Kuehne, "Techniques for measuring paraboloidal antennas," in "Design and Construction of Large Steerable Aerials," *IEE Conf. Pub.* No. **21**, 1966, pp. 187-198.

14. M. J. Puttock and H. C. Minnett, "Instrument for rapid measurement of surface deformations of a 210 ft radio telescope," *Proc. IEE*, **113**, 1966, pp. 1723-1730.

15. J. W. M. Baars and B. G. Hooghoudt, "The Synthesis Radio Telescope at Westerbork. General Lay-out and Mechanical Aspects," *Astron. & Astrophys.*, **31**, 1974, pp. 323-331.

16. J. M. Payne, "An optical distance measuring instrument," *Rev. Sci. Instrum.*, **44**, 1973, pp. 304-306.

17a. A. Greve and W. Harth, "Laser-diode distance meter in a theodolite," *Proc. Soc. Photo-Opt. Inst. Eng*, **236**, 1980, pp. 110-112.

17b. A. Greve and W. Harth, "Laser-diode distance meter in a KERN DKM 3A theodolite," *Applied Optics* **23**, 1984, pp. 2982-2984.

18. D. B. Shenton and R. E. Hills, "A proposal for a United Kingdom Millimetre Wavelength Astronomy Facility," Science Research Council, London, 1976.

19. C. Holst, A. Nothnagel, M. Blome, P. Becker, M. Eichborn and H. Kuhlmann, "Improved area-based deformation analysis of a radio telescope's main reflector based on terrestrial laser scanning," *J. of Applied Geodesy*, **9**, 2014, pp. 1-13.

20. R. Prestage, F. Schwab, and J. Shelton, "New Surface Measurement System," *Metrology and Control of Large Telescopes*, NRAO Green Bank Workshop, 2016 (accessible at nrao.edu).

21. K. Lau, H. Qiao and H. Song, "Design and testing of the API real-time metrology system for FAST," *Metrology and Control of Large Telescopes*, NRAO Green Bank Workshop, 2016.

22. J. M. Payne, J. M. Hollis and J. W. Findlay, "New method of measuring the shape of precise antenna reflectors," *Rev. Sci. Instrum.*, **47**, 1976, pp. 50-53.

23. J. W. Findlay and J. N. Ralston, "Testing the stepping method on the 140-ft telescope," *NRAO mm-telescope memos*, No. **94**, 1977.

24. R. Leighton, "A 10-meter telescope for millimeter and sub-millimetere astronomy," *Technical Report California Inst. Techn.*, 1978, 84 pages.

25. D. Woody, D. Vail and W. Schaal, "Design, construction and performance of the Leighton 10.4-m-diameter radio telescopes," *Proc IEEE*, **82**, 1994, pp. 673-686.

26. J. W. Findlay, "Operating experience at the National Radio Astronomy Observatory," *Annals of the New York Academy of Sciences*, **116**, Art.1, 1964, pp. 25-40.

27. C. S. Fraser, "Photogrammetric Measurement of Microwave Antennas," GSI Technical Report No. **86-001**, 1986, 30 pp.

28. K. Edmundson and L. Baker, "Photogrammetric measurement of the Arecibo primary reflector surface," *Coordinate Measurement Systems Committee Conference*, Albuquerque, 2001, 5 pp.

29. VertexRSI, "ALMA-US Prototype Antenna Photogrammetric Measurements," *Report*, Nov. 2002

30. R. Hills and F. Schwab, "Preliminary results from photogrammetry," unnumbered internal ALMA Note, January 2005, 5 pp.

31. D. Gale, D. Smith, A. Huerta, C. Torres, E. Rios, D. Santos, G. Valsecchi, R. Bianucci, "Post-fabrication metrology and analysis of the LMT segmented secondary reflector," *Proc. SPIE Advances in Optical and Mechanical Technologies for Telescopes and Instrumentation III*, **10706**, 2018, p. 10706.

32. D. Gale, F. Schloerb, A. Huerta, M. Álvarez, L. Cuevas, E. Sosa, D. Santos, C. Torres, E. Rios, "Photogrammetry mapping and alignment of the LMT 50-meter primary reflector," *Proc. SPIE Advances in Optical and Mechanical Technologies for Telescopes and Instrumentation III*, **10706**, 2018, p. 1070646.

33. R. Subrahmanyan, "Photogrammetric measurement of the gravity deformation in a Cassegrain antenna," *IEEE Trans. Ant. Prop.*, **53**, 2005, pp. 2590-2596.

34. F. Buffa, A. Causin, A. Cazzani, S. Poppi, G. Sanna, M. Solci, F. Stochino, and E. Turco "The Sardinia Radio Telescope: A comparison between close-range photogrammetry and finite element models," *Mathematics and Mechanics of Solids*, **22**, 2017, pp. 1005-1026.

35. R. C. Jennison, "*Introduction to Radio Astronomy*," Newnes London, 1966, 159 pages.

36. P. G. Smith, "Measurement of the Complete Far-Field Pattern of Large Antennas by Radio-Star Sources," *IEEE Trans. Antennas and Propagation*, **AP-14**, 1966, pp. 6-16.

37. A. P. Hartsuijker, J. W. M. Baars, S. Drenth, L. Gelato-Volders, "Interferometric measurement at 1415 MHz of radiation pattern of paraboloidal antenna at Dwingeloo radio observatory," *IEEE Trans. Antennas and Propagation*, **AP-20**, 1972, pp. 166.

38. J. W. Findlay and S. von Hoerner, "A 65-meter telescope for millimeter wavelengths," *National Radio Astronomy Observatory*, 1972, p. 40.

39. R. H. Bates, "Holographic approach to radiation pattern measurement -I- General theory," *Int. J. Engng Sci.*, **9**, 1971, pp. 1107-1121.

40. P. J. Napier and R. H. Bates, "Holographic approach to radiation pattern measurement -II- Experimental verification," *Int. J. Engng Sci.*, **9**, 1971, pp. 1193-1208.

41. J. C. Bennett, A. P. Anderson, P. A. McInnes, A. J. T. Whitaker, "Microwave holographic metrology of large reflector antennas," *IEEE Trans. on Antennas and Propagation*, **AP-24**, 1976, pp. 295-303.

42. P. F. Scott and M. Ryle, "A rapid method for measuring the figure of a radio telescope reflector," *Monthly Notices of the Royal Astronomical Society*, **178**, 1977, pp. 539-545.

43. D. Morris, "Phase retrieval in the radio holography of reflector antennas and radio telescopes," *IEEE Trans. Antennas Propagat.*, **AP-33**, 1985, pp. 749-755.

44. D. Morris, J. W. M. Baars, H. Hein, H. Steppe, C. Thum and R. Wohleben, "Radio-holographic reflector measurement of the 30-m Millimeter Radio Telescope at 22 GHz with a cosmic signal source," *Astron. Astrophys.*, **203**, 1988, pp. 399-406.

45. M. P. Godwin, E. P. Schoessow and B. H. Grahl, "Improvements in the Effelsberg 100 meter telescope based on holographic reflector surface measurements," *Astron Astrophys.*, **167**, 1986, p. 390.

46. D. Morris, M. Bremer, et al., "Surface adjustment of the IRAM 30 m radio telescope," *IET Microwaves, Antennas & Propagation*, **3**, 2009, pp. 99-108.

47. J. A. López-Pérez, P. de Vicente Abad, J. A. López-Fernández, F. Tercero, A. Barcia and B. Galocha, "Surface accuracy improvement of the Yebes 40-m radio telescope using microwave metrology," *IEEE Trans. Antennas and Propagation*, **AP-62**, 2014, pp. 2624-2633.

48. T. Hunter, F. R. Schwab, S. D. White, J. M. Ford, F. D. Ghigo, R. J. Maddalena, B. S. Mason, J. D. Nelson, R. M. Prestage, J. Ray, P. Ries, R. Simon, S. Srikanth and P. Whiteis, "Holographic Measurement and Improvement of the Green Bank Telescope Surface," *Publ. Astron. Soc. Pacific*, **123**, 2011, pp. 1087-1099.

49. J. W. M. Baars, R. N. Martin, J. G. Mangum, J. P. McMullin, W. L. Peters, "The Heinrich Hertz Telescope and the Submillimeter Telescope Observatory," *Publ. Astron. Soc. Pacific*, **111**, 1999, pp. 627-646.

50. Y. Rahmat-Samii, "Surface diagnosis of large reflector antenna using microwave holographic metrology: an iterative approach," *Radio Science*, **19**, 1984, pp. 1205-1217.

51. D. S. Rochblatt and B. L. Seidel, "Microwave Antenna Holography," *IEEE Trans. Microwave Theor. and Techn.*, **40**, 1991, pp. 1294-1300.

52. D. J. Rochblatt, "Microwave Antenna Holography," in M. S. Reid (ed.), *Low-Noise Systems in the Deep Space Network*, 2008, Chapter 8, pp. 323-360; JPL Descanso Book Series, vol. 10.

53. C. E. Mayer, F. H. Davis, W. L. Peters and W. J. Vogel, "A holographic surface measurement of the Texas 4.9 m antenna at 86 GHz," *IEEE Trans. Instrum. Meas.*, **IM-32**, 1983, pp. 102-109.

54. D. Morris, "Telescope testing by radio holography," International Symposium on Millimeter and Submillimeter Wave Radio Astronomy, Granada, URSI Publication, 1984, pp. 29-50.

55. I. A. Smith, F. Baas, F. Olivera, N. P. Rees, Y. Dabrowski, R. Hills, J. Richer, H. Smith and B. Ellison, "The New JCMT Holographic Surface Mapping System – Implementation," *Astronomical Data Analysis Software and Systems X*, ASP Conference Proceedings, **238**, 2001, p. 93.

56. J. W. M. Baars, R. Lucas, J. G. Mangum and J. A. Lopez-Perez, "Near-field radio holography of large reflector antennas," *IEEE Antennas and Propagation Magazine*, **49**, 2007, No. 5, pp. 24-41.

57. D. L. Misell, "A method for the solution of the phase problem in electron microscopy," *J. Appl. Phys. D*, **6**, 1973, pp. 16-19.

58. D. Morris, H. Hein, H. Steppe and J. W. M. Baars, "Phase retrieval radio holography in the Fresnel region: Tests on the 30-m telescope at 86 GHz," *IEE Proceedings*, **135**, Pt. H, 1988, pp. 61-64.

59. B. Nikolic, R. E. Hills and J. S. Richter, "Measurement of antenna surfaces from in- and out-of-focus beam maps

using astronomical sources," *Astron & Astrophys*, **465**, 2007, pp. 679-683.

60. B. Nicolic, R. M. Prestage, D. S. Balser, C. J. Chandler and R. E. Hills, "Out-of-focus holography at the Green Bank Telescope," *Astron & Astrophys*, **465**, 2007, pp. 685-693.

61. A. Greve, M. Bremmer, J. Peñalver, P. Rafin and D. Morris, "Improvement of the IRAM 30-m telescope from temperature measurements and finite element calculations," *IEEE Trans. Antennas and Propag.*, **AP-53**, 2005, pp. 851-860.

62. J. Ellder, L. Lundahl, D. Morris, "Test of phase-retrieval holography on the Onsala 20 m radiotelescope," *Electron. Lett.*, **20**, 1984, pp. 709-710.

63. J. W. M. Baars, *The Paraboloidal Reflector Antenna in Radio Astronomy and Communication*, Springer Astrophysics and Space Science Library, **348**, 2007, pp 166-167.

64. E. Serabyn, T.G. Phillips and C.R. Masson, "Surface figure measurements of radio telescopes with a shearing interferometer," *Appl. Optics*, **30**, 1991, pp. 1227-1241.